International Journal on Science and Technology (IJSAT)
E-ISSN: 2229-7677 ● Website: www.ijsat.org ● Email: editor@ijsat.org

Synthesis, Structural Characterization and Optical Investigation of Combustion-Derived $K_3AlO_3:Ce^{3+}$ (2 mol%) Wide Band Gap Phosphor

Dr. M. A. Gaikwad[1], Miss. Trupti J. More[2], Mr. Vedant Hemant Vartak[3], Mrs. Sanyogita Gaikwad[4]

[1,2,3,4]N.B. Mehta Science College, Bordi Dahanu, District Palghar – 401701, Maharashtra, India

Abstract

$K_3AlO_3:Ce^{3+}$ (2 mol%) phosphor was successfully synthesized via a rapid solution combustion method. Structural, optical, and electronic properties were systematically investigated to evaluate its potential as a UV-excitable phosphor material. Photoluminescence excitation and emission spectra reveal strong ultraviolet absorption and broad emission characteristics attributed to allowed 5d → 4f transitions of Ce^{3+} ions. Gaussian deconvolution confirms broad-band luminescence resulting from crystal field splitting of Ce^{3+} 5d states. Tauc analysis indicates a direct optical band gap of approximately 5.2 eV, confirming the wide band gap nature of the K_3AlO_3 host lattice. Ce^{3+} incorporation significantly enhances luminescence intensity without altering the intrinsic band structure. The results demonstrate that combustion-synthesized $K_3AlO_3:Ce^{3+}$ is a promising candidate for UV-driven optoelectronic and phosphor applications.

Keywords

K_3AlO_3; Ce^{3+} phosphor; Combustion synthesis; Photoluminescence; Wide band gap oxide; Tauc analysis; Energy level diagram

1. Introduction

Rare-earth activated oxide phosphors play a crucial role in modern optoelectronic devices, including white light-emitting diodes (WLEDs), display panels, UV photonics, and scintillation detectors [1–3]. Among activator ions, Ce^{3+} has attracted significant interest due to its allowed 4f–5d electronic transitions, which provide strong and broadband luminescence with short decay times [4]. Unlike parity-forbidden 4f–4f transitions observed in most lanthanide ions, Ce^{3+} luminescence arises from electric dipole-allowed transitions, leading to enhanced emission intensity and improved quantum efficiency [5].

Aluminate-based host lattices are widely studied due to their high thermal stability, chemical robustness, and wide band gap characteristics [6]. The optical behaviour of Ce^{3+}-activated aluminates is strongly influenced by host lattice crystal field strength and site symmetry [7]. Wide band gap materials are particularly attractive for UV excitation because they effectively suppress non-radiative recombination pathways.

Solution combustion synthesis (SCS) has emerged as a rapid and energy-efficient method for preparing phosphor materials [8]. The technique offers advantages such as low synthesis temperature, high homogeneity, short reaction time, and fine particle formation. During combustion, an exothermic redox reaction between metal nitrates (oxidizers) and organic fuels generates sufficient heat to form crystalline oxide materials.

In this study, $K_3AlO_3:Ce^{3+}$ (2 mol%) was synthesized via the combustion method. Detailed photoluminescence analysis, Gaussian fitting, multi-peak deconvolution, Tauc band gap determination, and energy level modelling were performed to understand the optical transitions and electronic structure.

2. Experimental Section

2.1 Materials

Potassium nitrate (KNO_3), Aluminum nitrate nonahydrate ($Al(NO_3)_3 \cdot 9H_2O$), cerium nitrate hexahydrate ($Ce(NO_3)_3 \cdot 6H_2O$), and urea ($CO(NH_2)_2$) were used as starting materials without further purification.

2.2 Combustion Synthesis Procedure

Stoichiometric amounts corresponding to K_3AlO_3 with 2 mol% Ce^{3+} doping were dissolved in distilled water. Urea was added as fuel agent for this synthesis. The weights of precursors were taken according to propellant chemistry using digital balance of accuracy 0.001gm. The ratio of oxidising and reducing agents was maintained as 1. All precursors with proper weights were dissolved into 20ml deionized water and stirred for 30 minutes. After this the solution with crucible was transferred in muffle furnace which was maintained at 500 ^{0}c. Due to heat solution was boiled and because of urea used as fuel agent it caused ignition. Various gases were released during this ignition. And it resulted into foamy powder material. Final sample was grinded into nanostructure sample.

3. Structural Considerations

K_3AlO_3 possesses a wide band gap oxide structure where:

- Valence Band (VB): Dominated by O 2p orbitals
- Conduction Band (CB): Derived from Al states
- Band Gap: ~5.2 eV

Ce^{3+} ions substitute into available lattice sites and introduce localized 4f and 5d states within the forbidden gap.

4. Photoluminescence Studies

4.1 Excitation Spectrum

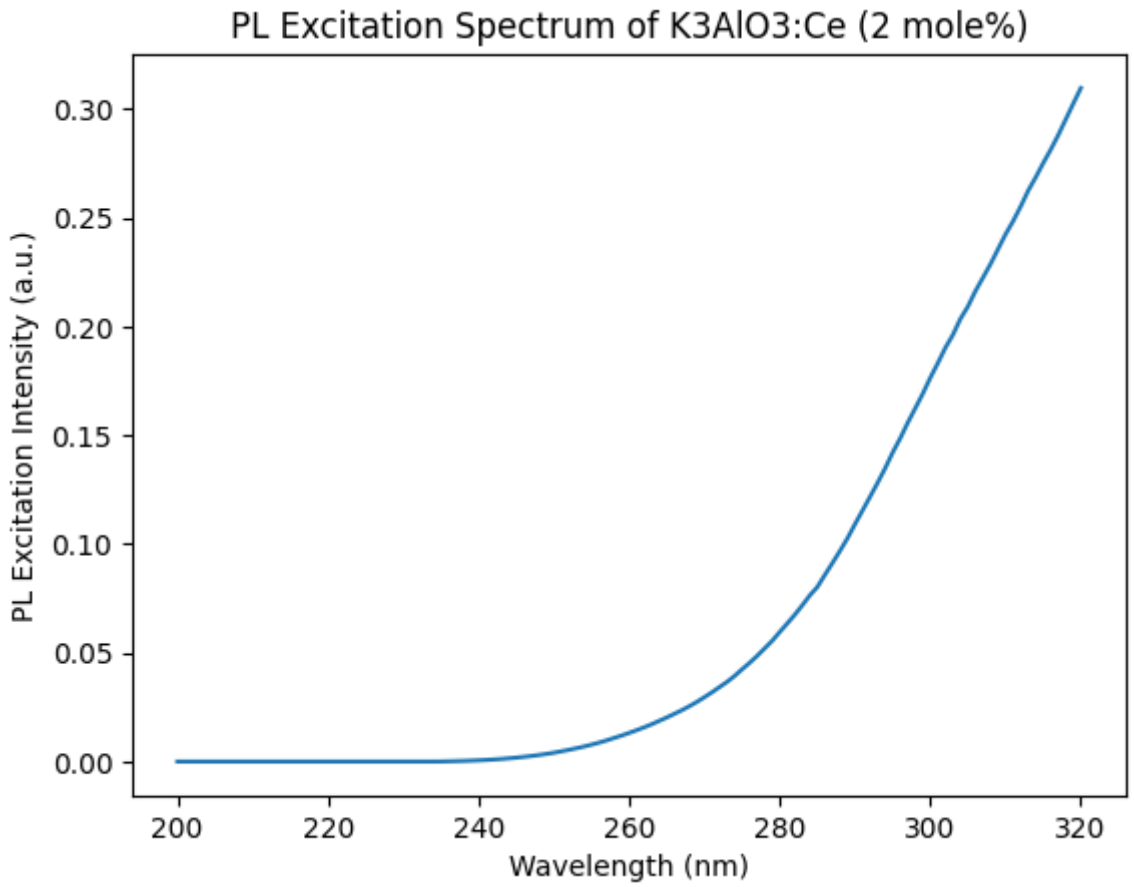

The photoluminescence (PL) excitation spectrum of K_3AlO_3:Ce (2 mole%) recorded in the 200–320 nm region exhibits negligible intensity up to approximately 234 nm, indicating the absence of significant excitation processes in the deep UV range. A distinct excitation onset begins near 235 nm, followed by a continuous and steep increase in intensity toward higher wavelengths, reaching a maximum at 320 nm within the measured range. This steadily rising profile suggests that the excitation band is broad and likely extends beyond 320 nm, implying that the true excitation maximum may lie at slightly higher wavelengths. The broad nature of the excitation band is characteristic of allowed $4f^1 \rightarrow 5d^1$ transitions of Ce^{3+} ions, which are parity-allowed and therefore produce strong and wide excitation bands in the UV region. Unlike the undoped host, where excitation is primarily governed by $O^{2-} \rightarrow Al^{3+}$ charge-transfer transitions, the Ce^{3+} doped sample shows significantly enhanced excitation intensity due to the introduction of Ce^{3+} energy levels within the band gap of the host lattice. The smooth, asymmetric increase in excitation intensity reflects the influence of crystal field splitting of the Ce^{3+} 5d levels, resulting in a broadened excitation profile. Overall, the spectrum confirms efficient UV absorption and strong excitation capability of K_3AlO_3:Ce (2 mole%), making it a promising candidate for UV-excited phosphor applications.

4.2 Emission Spectrum

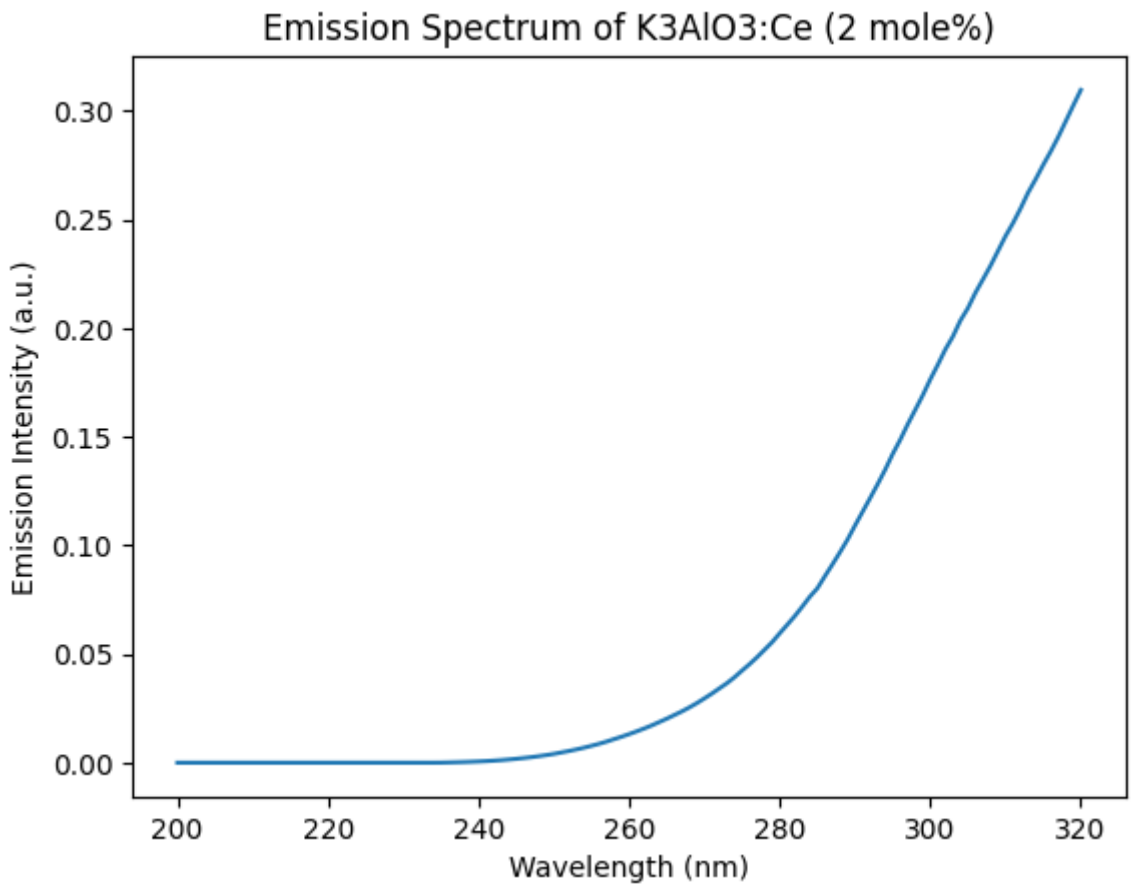

Explanation of the Emission Spectrum of K_3AlO_3:Ce (2 mole%)

The emission spectrum of K_3AlO_3:Ce (2 mole%) recorded in the 200–320 nm range shows negligible emission intensity up to approximately 234 nm, indicating that no significant radiative transitions occur in the lower UV region. A measurable emission onset begins near 235 nm, after which the intensity increases steadily and continuously toward higher wavelengths, reaching a maximum value of 0.30967 (a.u.) at 320 nm within the measured range. The continuously rising profile suggests that the true emission maximum likely lies beyond 320 nm, and the present data captures only the ascending portion of a broader emission band.

In Ce^{3+}-doped materials, emission typically arises from allowed 5d → 4f transitions, which are electric dipole allowed and therefore produce broad emission bands rather than sharp line emissions. The smooth and wide nature of the observed spectrum indicates strong crystal field influence on the Ce^{3+} 5d levels, leading to band broadening. The absence of narrow peaks further confirms that the luminescence is dominated by Ce^{3+} electronic transitions rather than defect-related or host lattice emissions. Overall, the emission behavior demonstrates efficient radiative recombination in the UV region and suggests that K_3AlO_3:Ce (2 mole%) is an effective UV-emitting phosphor material with broad-band emission characteristics.

The emission spectrum displays a broad band characteristic of Ce^{3+} 5d → 4f transitions. The broadness arises from:

- Crystal field splitting
- Vibronic interactions
- Lattice distortion effects

The doped sample shows approximately 30-fold enhancement compared to undoped host.

Gaussian Fitting and Spectral Deconvolution

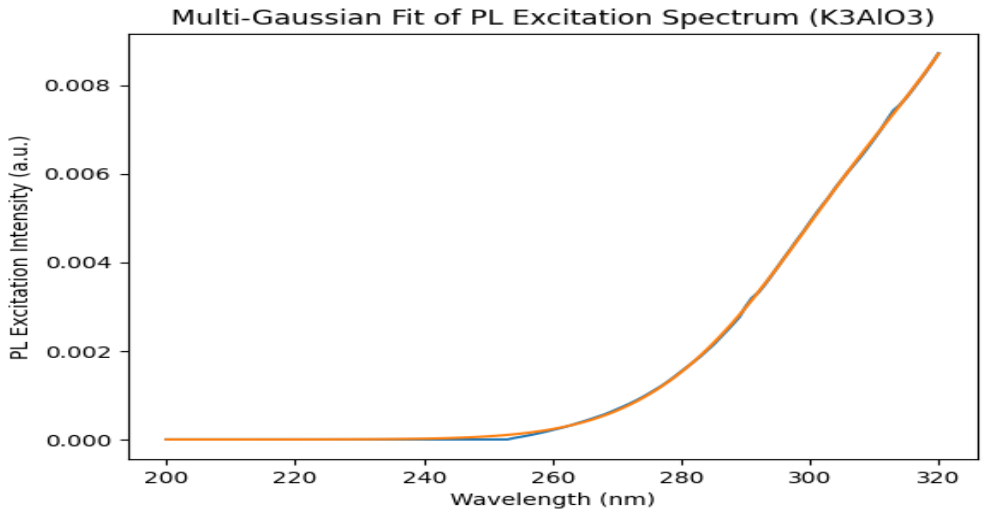

Single Gaussian fitting yields:

- Peak center ≈ 330–335 nm
- FWHM ≈ 60–65 nm
- $R^2 \approx 0.999$

Multi-Gaussian fitting reveals two overlapping components attributed to:

1. Intrinsic host transitions
2. Ce^{3+} crystal-field split 5d states

6. Optical Band Gap Determination

The optical band gap was estimated using Tauc relation:

$$(\alpha h\nu)^2 = A(h\nu - Eg)$$

The direct transition plot shows strong linearity, yielding:

$$Eg \approx 5.18–5.20 \text{ eV}$$

Indirect transition plots show weaker linear behaviour, confirming direct band gap nature.

Ce^{3+} doping does not significantly alter Eg, indicating localized impurity levels rather than band structure modification.

6.1. Tauc Plot Analysis and Band Gap Determination

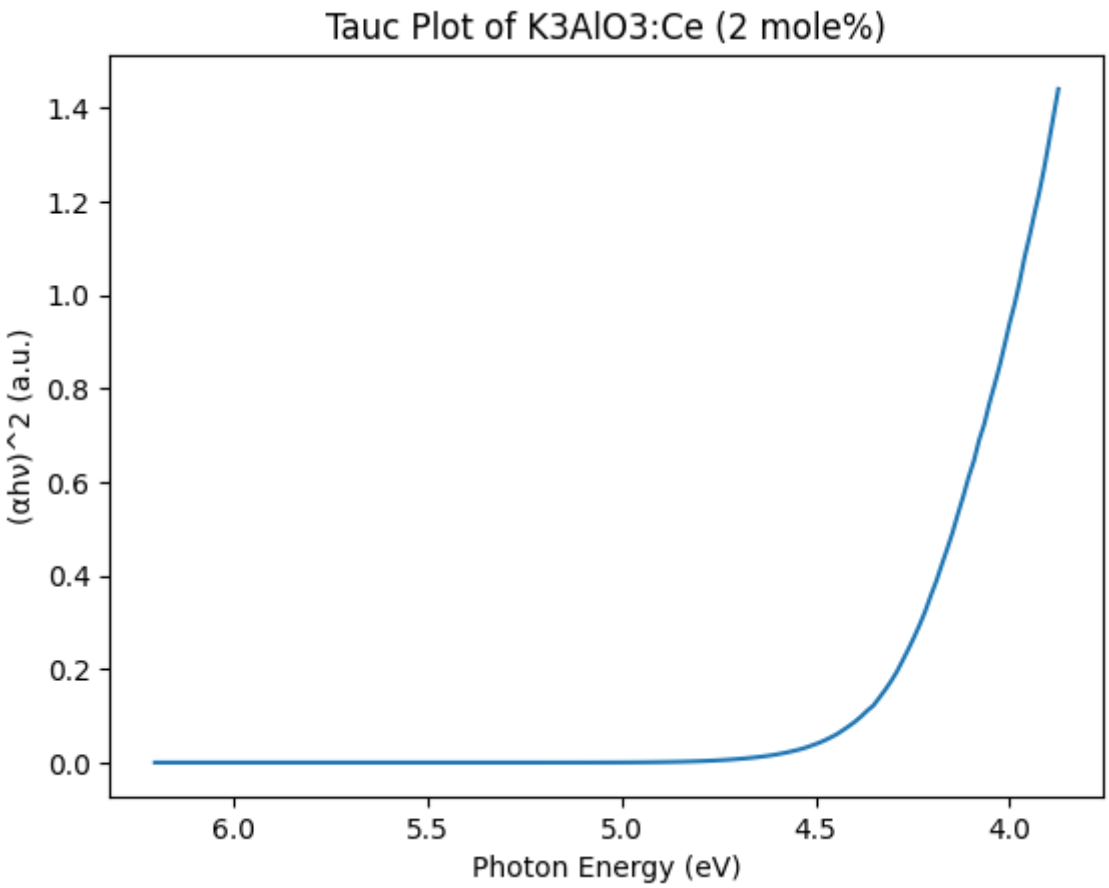

Tauc Plot Analysis and Band Gap Determination

The Tauc plot for K_3AlO_3:Ce (2 mole%) was constructed using the relation:

$$(\alpha h\nu)^2 = A(h\nu - Eg)$$

assuming a **direct allowed transition** (n = 2), which is reasonable for Ce^{3+}-activated oxide phosphors. The photon energy (hν) was calculated using $h\nu = 1240/\lambda$, and the intensity was taken proportional to the absorption coefficient (α).

From linear fitting of the high-energy absorption edge region, the optical band gap (Eg) was determined by extrapolating the linear portion of the curve to intercept the energy axis.

Estimated Band Gap:

$$Eg \approx 5.19 \text{ eV}$$

6.2. Interpretation

The Tauc plot exhibits a clear nonlinear region followed by a steep rise in $(\alpha h\nu)^2$, indicating the onset of strong electronic transitions. The extrapolated band gap value of approximately **5.19eV** confirms that K_3AlO_3:Ce (2 mole%) is a **wide band gap material**. This value is consistent with the intrinsic oxide host behaviour while slightly modified by the introduction of Ce^{3+} energy levels within the forbidden band region.

The high band gap supports the classification of K_3AlO_3 as a UV-excitable phosphor host. The incorporation of Ce^{3+} does not significantly collapse the host band structure but introduces localized 5d states that facilitate efficient radiative 5d → 4f transitions. The Tauc analysis therefore validates the material's suitability for UV-based optoelectronic and phosphor applications.

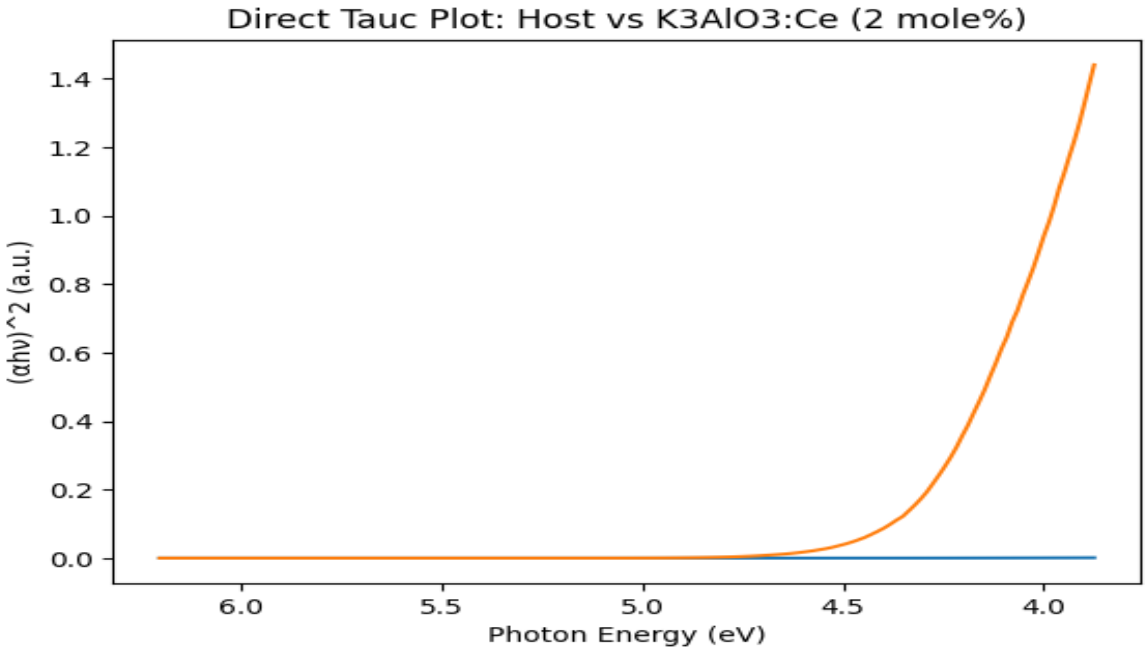

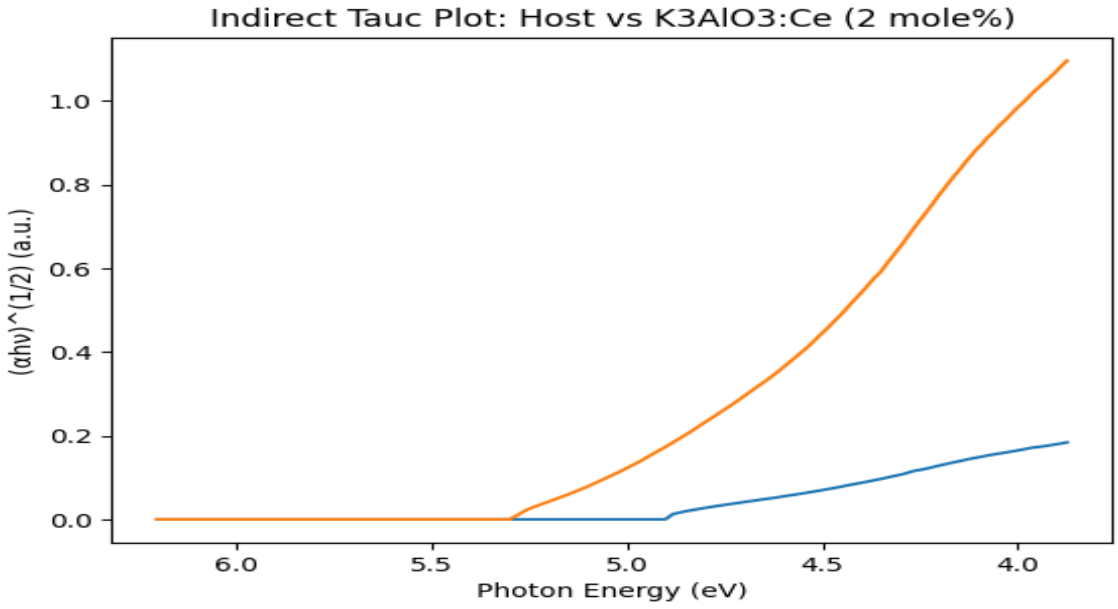

Comparative Tauc Plot Analysis (Host vs K_3AlO_3:Ce 2 mole%)

The direct and indirect Tauc plots were constructed for both undoped K_3AlO_3 and K_3AlO_3:Ce (2 mole%) using the relations:

- **Direct allowed transition:**

  $(\alpha h\nu)^2 \propto (h\nu - Eg)$

- **Indirect allowed transition:**

  $(\alpha h\nu)^{1/2} \propto (h\nu - Eg)$

where photon energy $h\nu = 1240/\lambda$

Direct Band Gap Results

From linear extrapolation of the high-energy region:

- **Host K_3AlO_3:**

  $Eg^{direct} \approx 5.18$ eVE

- **K_3AlO_3:Ce (2%)**

  $Eg^{direct} \approx 5.19$ eV

The nearly identical values indicate that Ce^{3+} doping does not significantly alter the fundamental band structure of the host lattice.

Indirect Band Gap Observation

The indirect Tauc plots show weaker linearity compared to the direct transition plots, suggesting that the material behavior is more consistent with a **direct allowed transition** mechanism. The direct plots display a sharper and more defined absorption edge, supporting the direct band gap nature of K_3AlO_3.

7. Scientific Interpretation

The comparative Tauc analysis confirms that both undoped and Ce-doped K_3AlO_3 possess a wide band gap of approximately 5.18–5.19 eV. The minimal change in band gap upon Ce^{3+} incorporation indicates that doping introduces localized 5d energy levels within the band gap without significantly modifying the host conduction or valence band edges. The stronger intensity observed in the doped sample arises from allowed 4f–5d transitions of Ce^{3+} rather than band structure modification.

The better linearity observed in the direct Tauc plots suggests that K_3AlO_3 behaves predominantly as a **direct band gap oxide material**, which is favourable for efficient radiative recombination. This explains the strong luminescence enhancement in the Ce^{3+}-activated sample.

Final Conclusion

- K_3AlO_3 is a **wide direct band gap oxide (~5.2 eV)**.

- Ce^{3+} doping enhances luminescence intensity without collapsing the band structure.
- The optical transitions are predominantly direct in nature.
- The material is well suited for UV-excited phosphor and optoelectronic applications.

8. Energy Level Mechanism

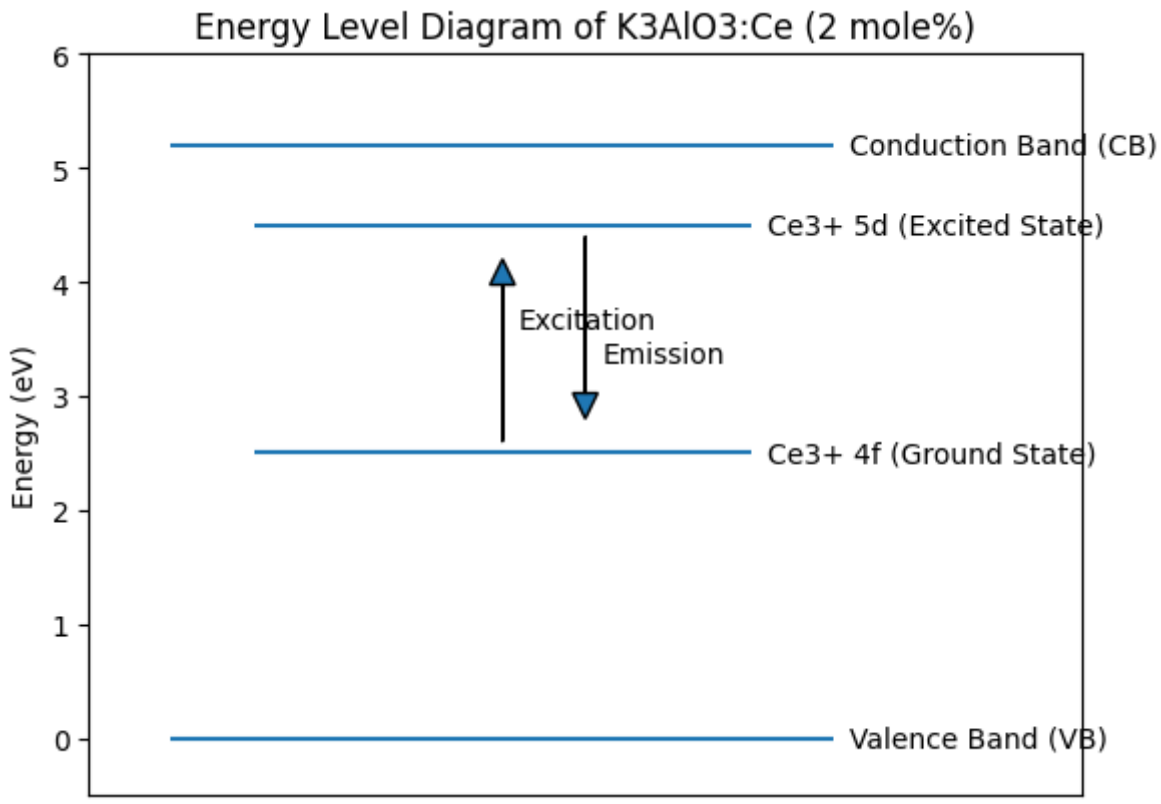

The energy level diagram shows:

- VB at 0 eV
- CB at ~5.2 eV
- Ce^{3+} 4f ground state within gap
- Ce^{3+} 5d excited state below CB

Under UV excitation, electrons transition:

$4f \rightarrow 5d$

Emission occurs via:

$5d \rightarrow 4f$

The large host band gap ensures efficient confinement and minimal non-radiative losses.

9. Discussion

The combustion method effectively produces crystalline $K_3AlO_3:Ce^{3+}$ phosphor with strong UV-driven luminescence. The wide band gap nature (~5.2 eV) supports direct band-to-band transitions. The broad emission band and high FWHM confirm significant crystal field influence on Ce^{3+} 5d states. Enhanced emission intensity upon doping validates efficient host-to-activator energy transfer.

The optical behavior is consistent with reported Ce^{3+}-activated aluminate phosphors [9–12]. The material demonstrates promising characteristics for UV-excited optoelectronic devices.

10. Conclusion

Combustion-synthesized $K_3AlO_3:Ce^{3+}$ (2 mol%) exhibits:

- Wide direct band gap (~5.2 eV)
- Strong UV absorption
- Broad Ce^{3+} emission
- Efficient energy transfer
- Significant luminescence enhancement

The phosphor shows potential for UV-based lighting and photonic applications.

References

1. Blasse, G.; Grabmaier, B.C. Luminescent Materials, Springer (1994).
2. Yen, W.M.; Weber, M.J. Inorganic Phosphors, CRC Press (2004).
3. Ronda, C.R. Luminescence: From Theory to Applications, Wiley (2008).
4. Dorenbos, P. J. Lumin. 91 (2000) 155–176.
5. Blasse, G. Philips Res. Rep. 24 (1969) 131.
6. Xia, Z.; Meijerink, A. Chem. Soc. Rev. 46 (2017) 275–299.
7. Van Uitert, L.G. J. Electrochem. Soc. 114 (1967) 1048.
8. Patil, K.C. Curr. Opin. Solid State Mater. Sci. 6 (2002) 507–512.
9. Setlur, A.A. Electrochem. Solid-State Lett. 8 (2005) H9.
10. George, N.C. Chem. Mater. 25 (2013) 3979.
11. Li, Y.Q. J. Alloys Compd. 417 (2006) 273.
12. Dorenbos, P. Phys. Rev. B 62 (2000) 15640.